Supplementary Information for:

Serendipitous Synthetic Entrée to Tetradehydro Analogues of Cobalamins

Richard M. Deans, Olga Mass, James R. Diers, David F. Bocian and Jonathan S. Lindsey

Table of Contents

1. Survey of Lewis Acids for Tetradehydrocorrin Formation

The formation of **2** was examined at room temperature in the presence of a Lewis acid ($InCl_3$, $Ga(OTf)_3$, or $Bi(OTf)_3$) in CH_2Cl_2. A 20 mM stock solution of each starting compound was prepared: a solution of **4-Br** (14.0 mg, 0.0335 mmol) in CH_2Cl_2 (1.68 mL), and a solution of **5b** (9.2 mg, 0.031 mmol) in CH_2Cl_2 (1.57 mL). A 250-μL aliquot of each stock solution was added to each of three 4-mL conical reaction vials, so that each vial contained 10 mM of **4-Br** (0.005 mmol per vial) and 10 mM of **5b** (0.005 mmol per vial). $InCl_3$ (2.21 mg, 0.01 mmol, 2 equiv) was added to the first vial, $Ga(OTf)_3$ (5.17 mg, 0.01 mmol, 2 equiv) was added to the second vial, and $Bi(OTf)_3$ (6.56 mg, 0.01 mmol, 2 equiv) was added to the third vial. The progress of the reaction was monitored by TLC [silica, CH_2Cl_2/hexanes (2:1)] at 10, 20, and 45 min. TLC plates were prepared by first quenching a 50-μL aliquot from each crude mixture with CH_2Cl_2/Et_3N (30 μL, 99:1). A 1-μL sample from each quenched aliquot was spotted onto a TLC plate. All three reactions were quenched with triethylamine (5 μL) after 1 h, whereupon the extent of formation of **2** was assessed using LD-MS and TLC. Compound **2** was detectable in all three samples by LD-MS (obsd m/z = 566.6). The relative efficacy of the acid conditions was determined via TLC by examining the intensity of the distinct green spot that is indicative of a tetradehydrocorrin macrocycle. Use of $InCl_3$ resulted in no visibly detectable spot, while use of $Bi(OTf)_3$ gave a very faint green spot (R_f = 0.64) that faded quickly. Use of $Ga(OTf)_3$ gave a strong, dark green spot (R_f = 0.64); thus, $Ga(OTf)_3$ in CH_2Cl_2 was identified as the best condition for formation of **2** from among those surveyed. No quantitative yields were determined as part of this preliminary study.

2. Acid Stability of 2

In a 4-mL conical reaction vial, **3** (5.10 mg, 0.008 mmol) in anhydrous CH_2Cl_2 (1.66 mL) was treated with TMSOTf (7.50 μL, 0.042 mmol, 5 equiv) at room temperature (Reaction 1). In a second 4-mL conical reaction vial, **2** (4.20 mg, 0.00741 mmol) in anhydrous CH_2Cl_2 (1.48 mL) was treated with TMSOTf (6.70 μL, 0.037 mmol, 5 equiv) at room temperature (Reaction 2).

The conversion of either tetradehydrocorrin species to bacteriochlorin was monitored by

TLC [alumina, hexanes/CH_2Cl_2 (2:1)] and UV-Vis absorption spectroscopy at 30 min, 1 h, 2 h, 4 h, 6 h, 22 h, and 24 h. TLC plates were prepared by quenching a 15-μL aliquot from each reaction vial with 5 drops of CH_2Cl_2/Et_3N (50:1). A 1-μL sample from each quenched aliquot was spotted onto a TLC plate. Each plate included pure samples of **BC-T$_2$**, **3**, and **2**. UV-Vis samples were prepared from each reaction by adding a 10-μL aliquot of the respective crude mixture to a cuvette containing 1.00 mL CH_2Cl_2. The solution in each cuvette was quenched by the addition of 1 drop of Et_3N.

During the first 6 h, TLC indicated the conversion of **3** to **BC-T$_2$** as the dark green **3** spot (R_f = 0.23) faded and the light green **BC-T$_2$** spot (R_f = 0.43) intensified. This observation was corroborated by UV-Vis spectroscopy, which showed a strong long-wavelength absorption band (Q_y(0,0) = 734 nm) characteristic of **BC-T$_2$**. In contrast, TLC and UV-Vis spectroscopy indicated that **2** did not convert to bacteriochlorin over the first 6 h of the experiment. The dark green **2** spot (R_f = 0.33) did not diminish significantly in intensity nor did a second green spot indicative of bacteriochlorin appear. The absorption spectral features in the region from 500–1000 nm lacked the strong long-wavelength absorption band (Q_y(0,0) > 700 nm) displayed by bacteriochlorins; rather, the absorption band in this region remained weak and broad as is characteristic of tetradehydrocorrin macrocycles.

When surveyed again at 22 h and 24 h, the remaining **3** and any **BC-T$_2$** (which had formed initially) appeared to have decomposed. The UV-Vis absorption spectrum showed neither the sharp absorption band at 734 nm characteristic of **BC-T$_2$** nor the broad absorption from 500–1000 nm characteristic of **3**.

When surveyed again at 22 h and 24 h, **2** also appeared to have largely decomposed. The UV-Vis absorption spectrum showed neither the distinctive long-wavelength absorption band (Q_y(0,0) > 700 nm) displayed by bacteriochlorins nor the broad absorption characteristic of tetradehydrocorrin macrocycles. After 24 h, Reaction 2 was quenched with aqueous $NaHCO_3$ (10 mL). The organic extract was dried (Na_2SO_4), concentrated, and analyzed by LD-MS, which showed multiple peaks indicating decomposition. This survey indicates that under acidic conditions, **2** is resistant to bacteriochlorin conversion and is relatively stable for at least 6 h.

3. ^{1}H NMR Characterization of 1 and 2

The ^{1}H NMR spectrum of **2** is relatively complex owing to the C_1 symmetry of the macrocycle. Accordingly, the three meso carbons (and protons attached thereto) are each unique, as are the four β-pyrrolic carbons and the two pyrroline CH_2 units. Distinctive spectral features include (i) an AB splitting pattern in the high-field region (δ 2.00 ppm, δ 2.24 ppm) assigned to the two methylene protons of the pyrroline unit; (ii) five distinct resonances in the range δ 5.53–6.66 ppm collectively assigned to the five peripheral alkenyl or β-pyrrolyl protons (attached at the 5-, 8-, 10-, 15-, and 18-positions); (iii) two doublets and a multiplet in the range δ 7.21–7.45 ppm collectively assigned to the eight aryl protons of the 7-(*p*-ethylphenyl) and 17-(*p*-tolyl) substituents; (iv) two broad resonances in the low-field region (δ 11.04–11.10 and δ 11.69–11.75) assigned to the two NH protons. These resonance assignments were inferred by comparing the ^{1}H NMR spectrum of **2** to the very similar ^{1}H NMR spectrum of **3**, for which complete resonance assignments were reported.[39] The ^{13}C NMR spectrum of **2** displays 35 signals, which is consistent with the proposed structure.

4. X-ray Crystal Structure of 2

The unit cell of **2** is composed of 16 molecules, which are present as a racemic mixture of the two enantiomers (arbitrarily designated A and B). The unit cell can be further divided into 4 quadrants each of which contains two A and two B enantiomers (Figure S1).

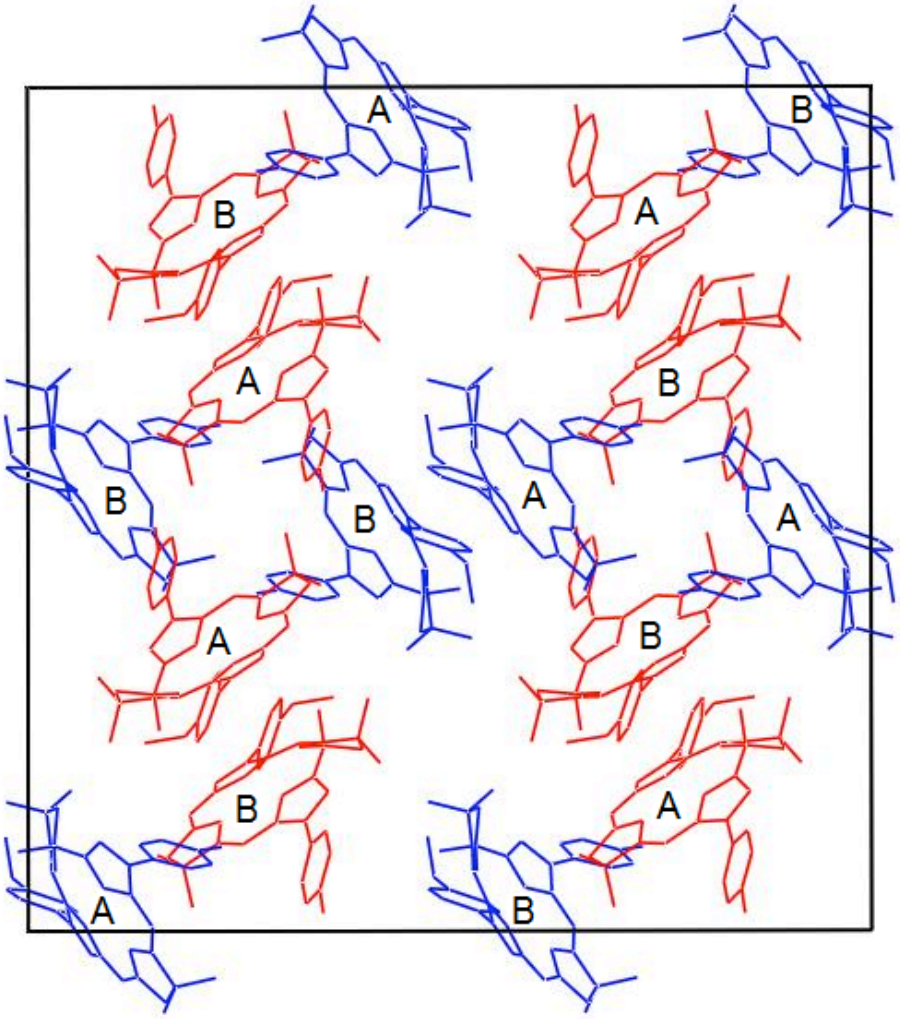

Figure S1. Unit cell of **2**. Proximal pairs are shown in red and distal pairs are shown in blue. Enantiomers are labeled either A or B.

Within each quadrant, one A and one B enantiomer are arranged as a closely spaced pair (the proximal pair) while the other A and B enantiomers are arranged as a distantly spaced pair (the distal pair) (Figure S2). The proximal pairs have the following properties: (i) when the four nitrogen atoms of each **2** molecule in a proximal pair are used to construct a plane, the respective planes defined by each enantiomer in the pair are exactly parallel (dihedral angle = 0°); (ii) the distance between the respective planes defined by each enantiomer in a pair is 2.707(2) Å; (iii) the planes defined by each enantiomer in the pair are staggered; (iv) the convex faces of the two enantiomers are oriented toward each other (Figure S2). A summary of the crystal data for the tetradehydrocorrin **2** is provided in Table S1.

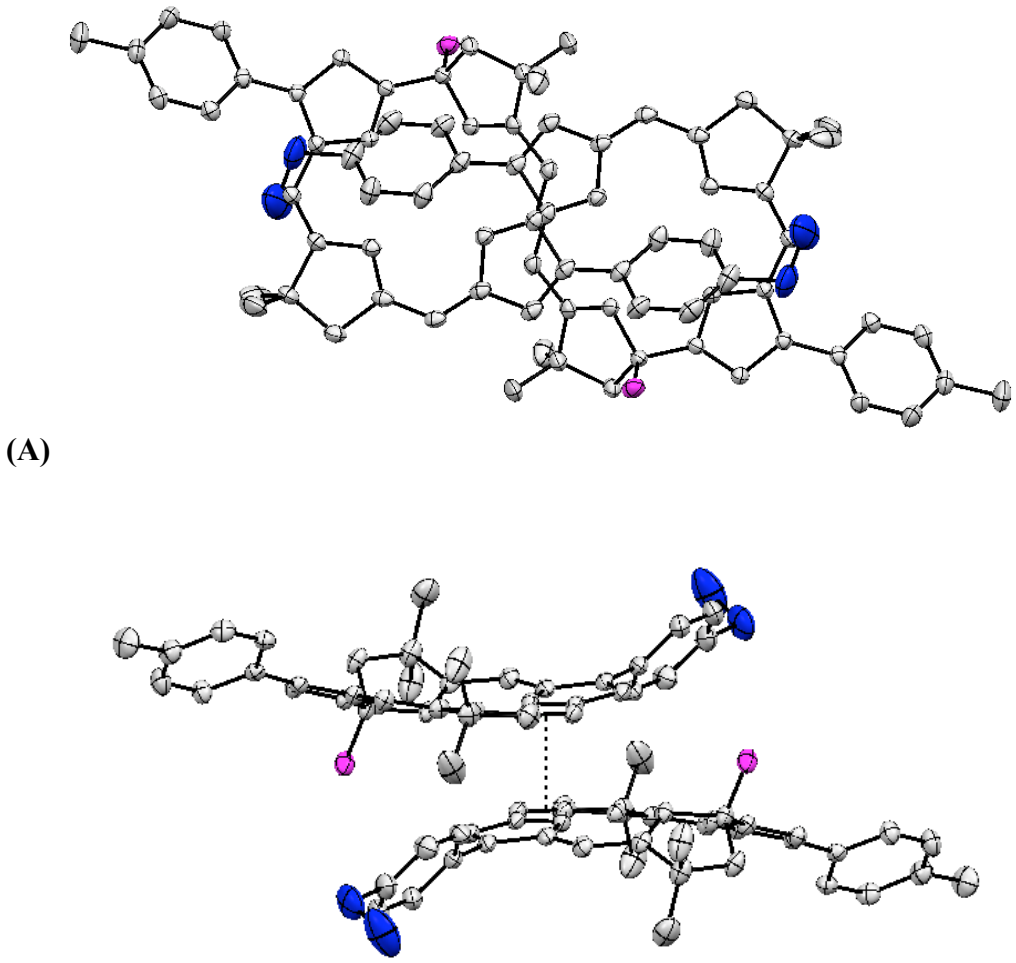

(A)

(B)

Figure S2. **(A)** Staggered overlap between the two enantiomeric members of a proximal pair. **(B)** Interplanar distance between members of a proximal pair (x, y, z and –x, -y, 1-z on bottom and top respectively). The interplanar distance shown is 2.707(2) Å (dashed line). Note that the 1-methyl carbons are shown in magenta and the ethyl carbons of the β-pyrrolic *p*-ethylphenyl substituents are shown in blue for clarity.

The chloroform solvent in this structure forms disordered channels around the 4_1 screw axis with a site occupancy of roughly 7%. The central C of the solvent was located as a peak in the difference map with a residual density of < 0.5 $e^-/Å^3$. The close approach of the chloroform H to the neighboring methyl hydrogen on C32 is likely the combined effect of the low occupancy of the solvent, the restraints placed on the C-Cl and Cl-Cl distances to maintain a chemically reasonable shape, and the calculated placement of the H atoms at fixed distances for both the solvent and methyl group. No substantive change in bond lengths or angles of the molecule of interest is evident when a more detailed model is attempted.

Table S1. Summary of Crystal Data for 2

Formula	$C_{39.07}H_{42.07}Cl_{0.22}N_4$
Formula Weight (*g/mol*)	575.59
Crystal Dimensions (*mm*)	0.50 × 0.47 × 0.37
Crystal Color and Habit	purple prism
Crystal System	tetragonal
Space Group	I 4_1/a
Temperature, K	110
a, Å	30.805(7)
b, Å	30.805(7)
c, Å	14.937(3)
α,°	90.00
β,°	90.00
γ,°	90.00
V, Å^3	14174(4)
Number of reflections to determine final unit cell	9730
Min and Max 2θ for cell determination, °	4.82, 61.08
Z	16
F(000)	4933
ρ (*g/cm*)	1.079
λ, Å, (MoKα)	0.71073
μ, (*cm^{-1}*)	0.080
Diffractometer Type	Bruker-Nonius Kappa Axis X8 Apex2
Scan Type(s)	omega and phi scans
Max 2θ for data collection, °	67.58
Measured fraction of data	0.991
Number of reflections measured	157107
Unique reflections measured	13754
R_{merge}	0.0374
Number of reflections included in refinement	13754
Cut off Threshold Expression	>2sigma(I)
Structure refined using	full matrix least-squares using F^2
Weighting Scheme	calc w=1/[sigma^2(F_o^2)+(0.0772P)^2+3.7230P] where P=(F_o^2+2F_c^2)/3
Number of parameters in least-squares	563
R_1	0.0530
wR_2	0.1321
R_1 (all data)	0.0963
wR_2 (all data)	0.1543
GOF	1.034
Maximum shift/error	0.001
Min & Max peak heights on final ΔF Map (*e$^-$*/Å)	-0.232, 0.556

Where:

$R_1 = \Sigma(|F_o| - |F_c|) / \Sigma F_o$

$wR_2 = [\Sigma(w(F_o^2 - F_c^2)^2) / \Sigma(w F_o^4)]^{1/2}$

GOF = $[\Sigma(w(F_o^2 - F_c^2)^2) /$ (No. of reflns. - No. of params. $)]^{1/2}$

5. Survey of Cobalt Reagents for Tetradehydrocorrin Metalation

A solution of **2** (4.0 mg, 0.0071 mmol, 2 mM) in MeOH/$CHCl_3$ [3.55 mL, (1:1)] was divided equally between two reaction vials. Anhydrous $Co(OAc)_2$ (12.6 mg, 0.071 mmol, 10 equiv) was added to the first vial under argon. Anhydrous $CoCl_2$ (9.22 mg, 0.071 mmol, 10 equiv) was added to the second vial under argon. The solution containing $Co(OAc)_2$ changed from dark green to purple-red within three min. The solution containing $CoCl_2$ changed from dark green to purple-red within a few sec. The reaction progress was monitored by TLC [silica, hexanes/CH_2Cl_2, (1:1)]. After 10 min, TLC indicated complete consumption of the starting material in both reactions. Water was added to both reactions after 25 min. The organic fraction from each reaction was dried (Na_2SO_4) and concentrated. The crude product from the $Co(OAc)_2$ reaction was a reddish-brown solid. The crude product from the $CoCl_2$ reaction was a purple-red solid. The crude product from each reaction was analyzed by LD-MS and ESI-MS. The LD-MS and ESI-MS spectra of each reaction product showed peaks consistent with cobalt insertion into the **2** macrocycle plus an axial hydroxide or methoxide ligand. Comparison of the ESI-MS spectra indicated the $CoCl_2$ reaction to be cleaner given the presence of fewer unidentified byproducts. Thus, treatment of **2** with 10 molar equivalents of either anhydrous $Co(OAc)_2$ or anhydrous $CoCl_2$ affords the corresponding cobalt–tetradehydrocorrin complex. Anhydrous $CoCl_2$ was used in all subsequent tetradehydrocorrin metalation experiments.

6. Examination of Cobalt Chelates by ^{1}H NMR Spectroscopy

A sample of **Co2-MeOH** was examined by ^{1}H NMR spectroscopy (300 MHz) under a variety of conditions. The ^{1}H NMR spectrum in CD_3OD at room temperature showed very broad peaks that afforded little structural insight, and the spectrum remained unchanged at lower temperatures (0 °C, –20 °C, –30 °C, –35 °C; examined at 400 MHz). The ^{1}H NMR spectrum in toluene-d_8 or $CDCl_3$ at room temperature was similarly uninformative. The ^{1}H NMR spectrum in pyridine-d_5 at room temperature gave much sharper peaks than the spectrum in CD_3OD, but none of the observed peaks could be definitively assigned.

7. Expanded Absorption Spectra for Co2-MeOH Titrations

The following spectra (A, B, D, E) are enlarged versions of those shown in Figure 5; Pathway C is shown here. The absorption spectral parameters of various compounds are shown in Table S2. The absorption spectral parameters during titrations are summarized in Table S3.

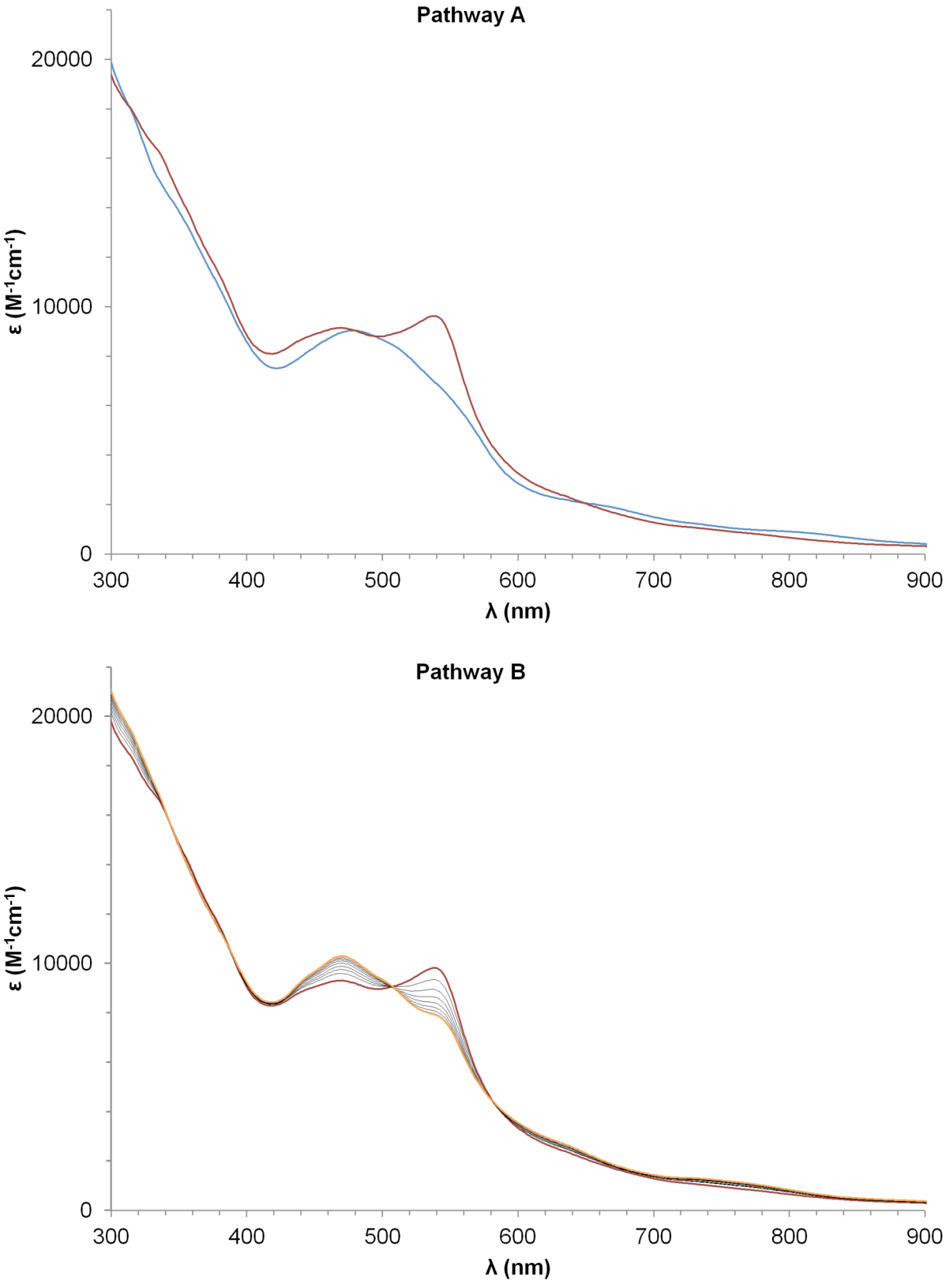

Figure S3. Pathways A and **B.**

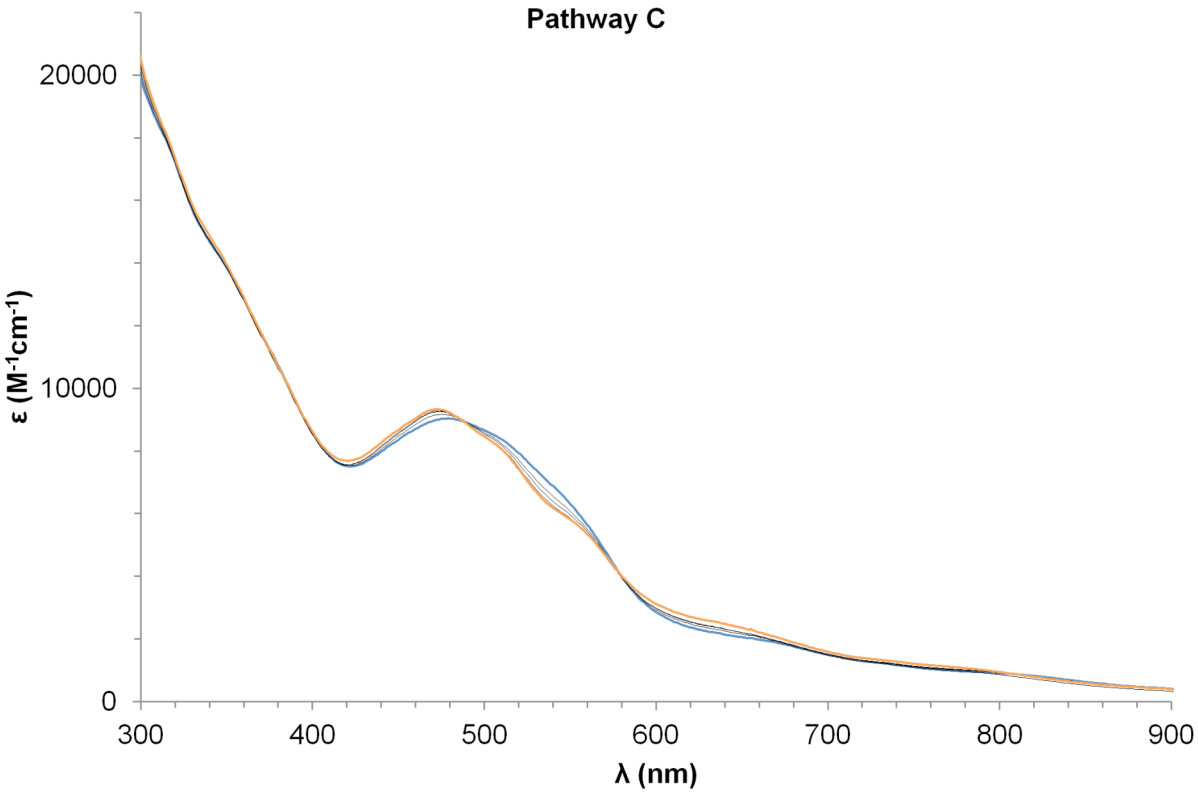

Figure S3. Pathway C. Titration of **Co2-THF** (blue line, sample derived from **Co2-MeOH**) with five 5-μL aliquots of methanol/pyridine (9:1) to give **Co2-pyr**. The titration was carried out with an initial concentration of 40 μM of **Co2-THF**.

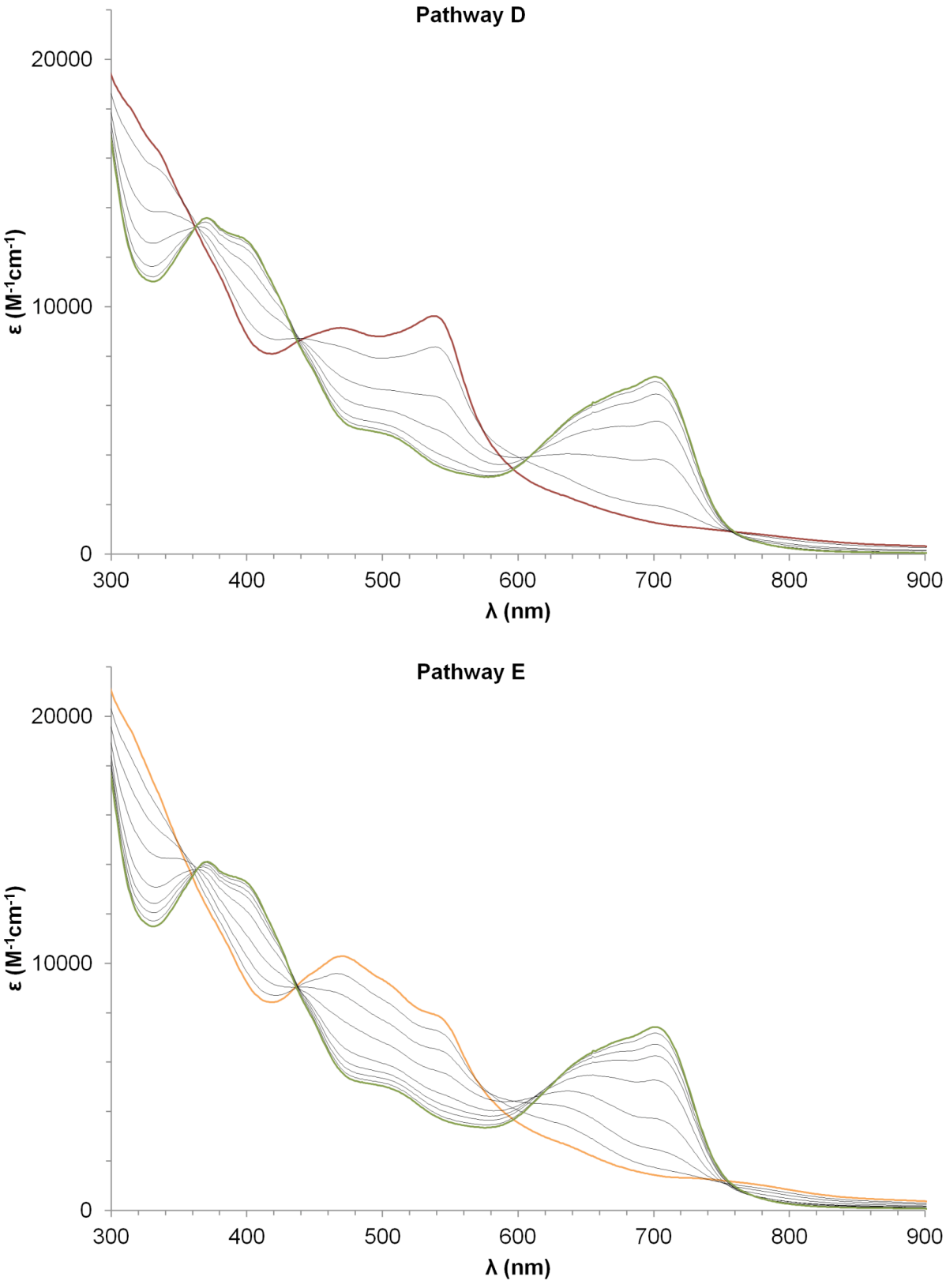

Figure S3. Pathways D and **E.**

Table S2. Summary of absorption spectral parameters of various compounds.

Compound	Major absorption bands (nm)
Co2-MeOH	469, 539 (λ_{max})
Co2-THF	479 (λ_{max})
Co2-pyr	470 (λ_{max}), 506 (sh), 540 (sh)
Co2-$(CN)_2$	371 (λ_{max}), 398, 509 (sh), 701

Table S3. Summary of absorption spectral parameters during titrations.

Pathway	Isosbestic Wavelengths (nm)
A	-
B	506, 582
C	487, 578
D	363,* 437, 758
E	362,* 436, 755*

* imprecise curve overlap (i.e., not an isosbestic point) indicates the presence of >2 species.

8. Chromatographic Separation of Co–Tetradehydrocorrin Sample

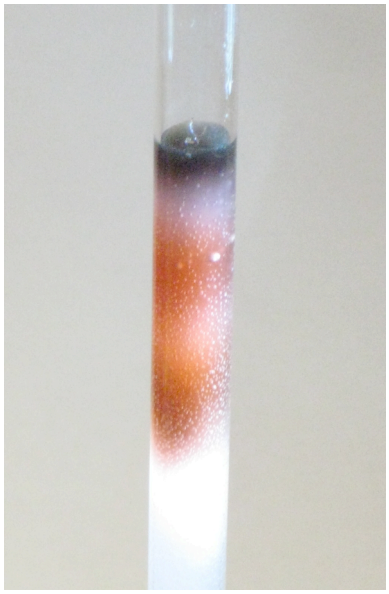

Figure S4. Chromatographic separation of putative diastereomers of **Co2-MeOH** in a pipette column.

9. IR Spectral Data

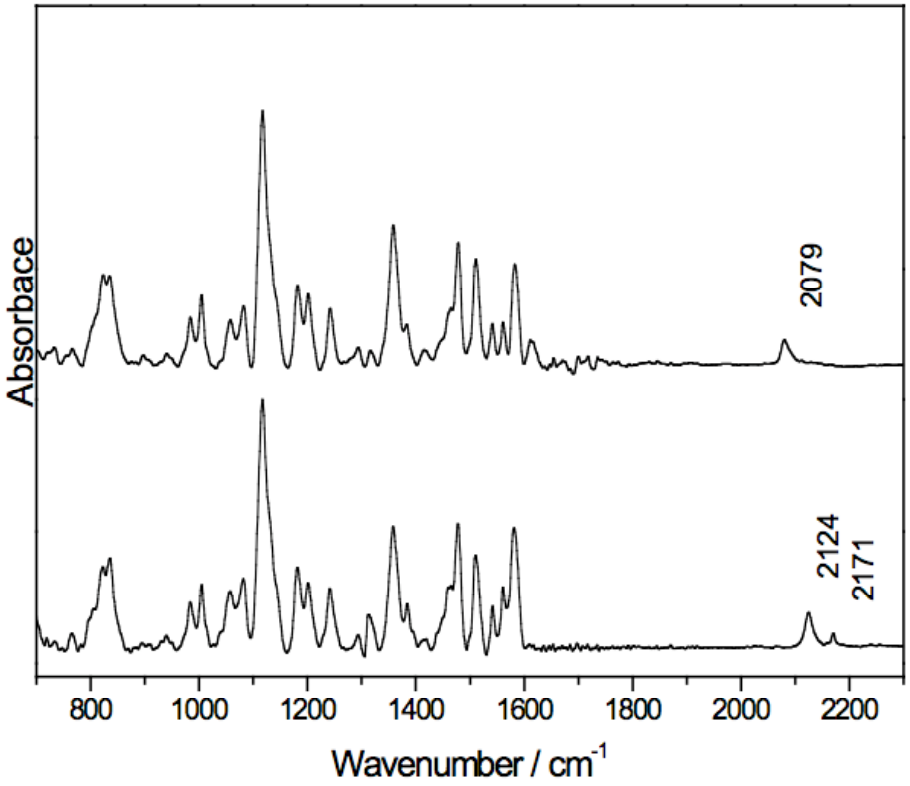

Figure S5. FTIR spectrum (KBr pellet) of **Co2-(^{13}CN)$_2$** (upper) and of **Co2-(CN)$_2$** (lower).

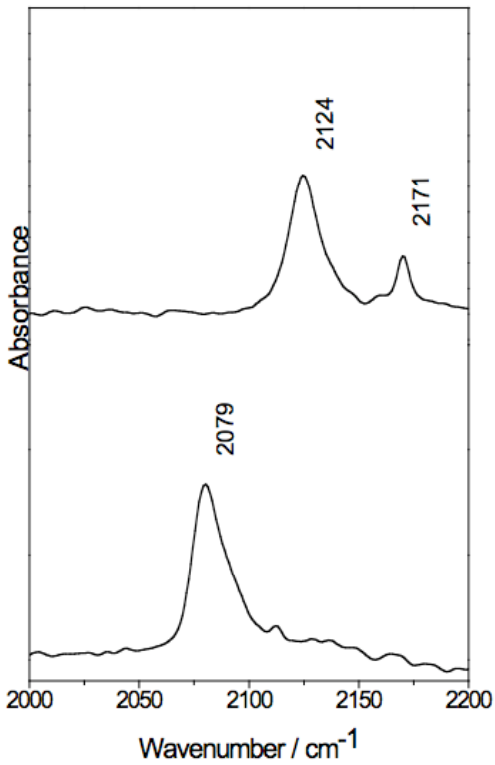

Figure S6. Expanded region of the FTIR spectrum (KBr pellet) of **Co2-(CN)$_2$** (upper) and of **Co2-(^{13}CN)$_2$** (lower).

10. NMR Spectral Data

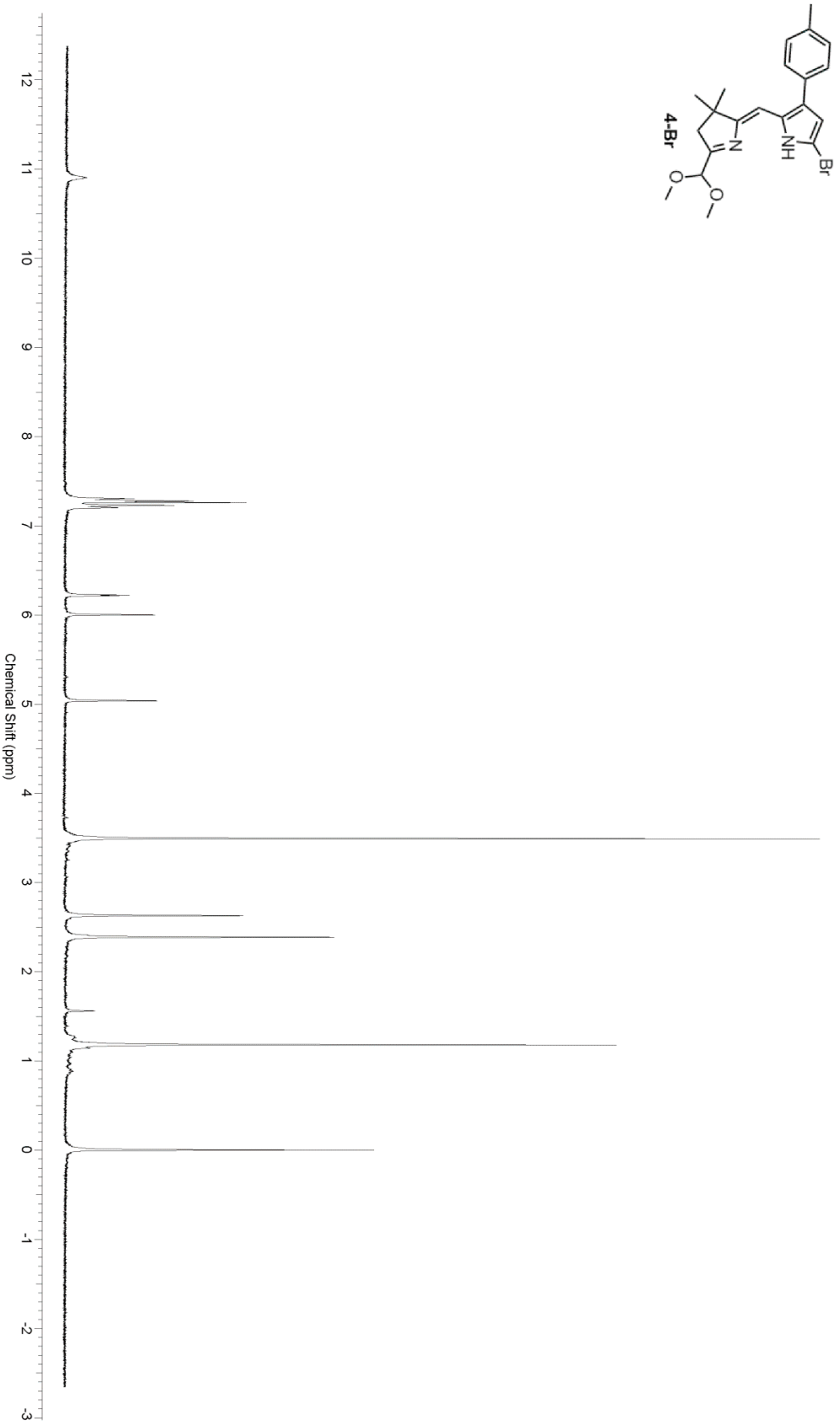

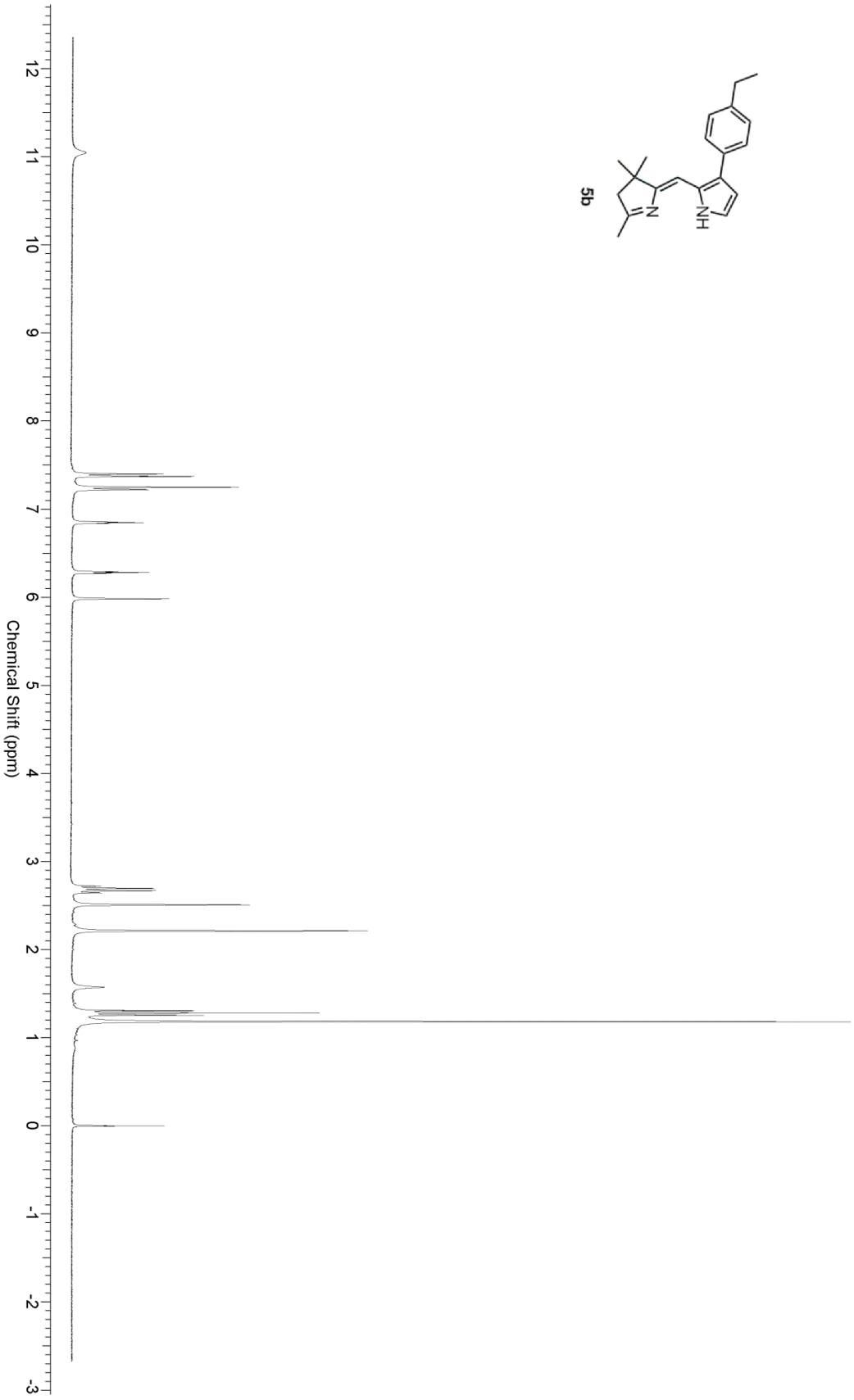

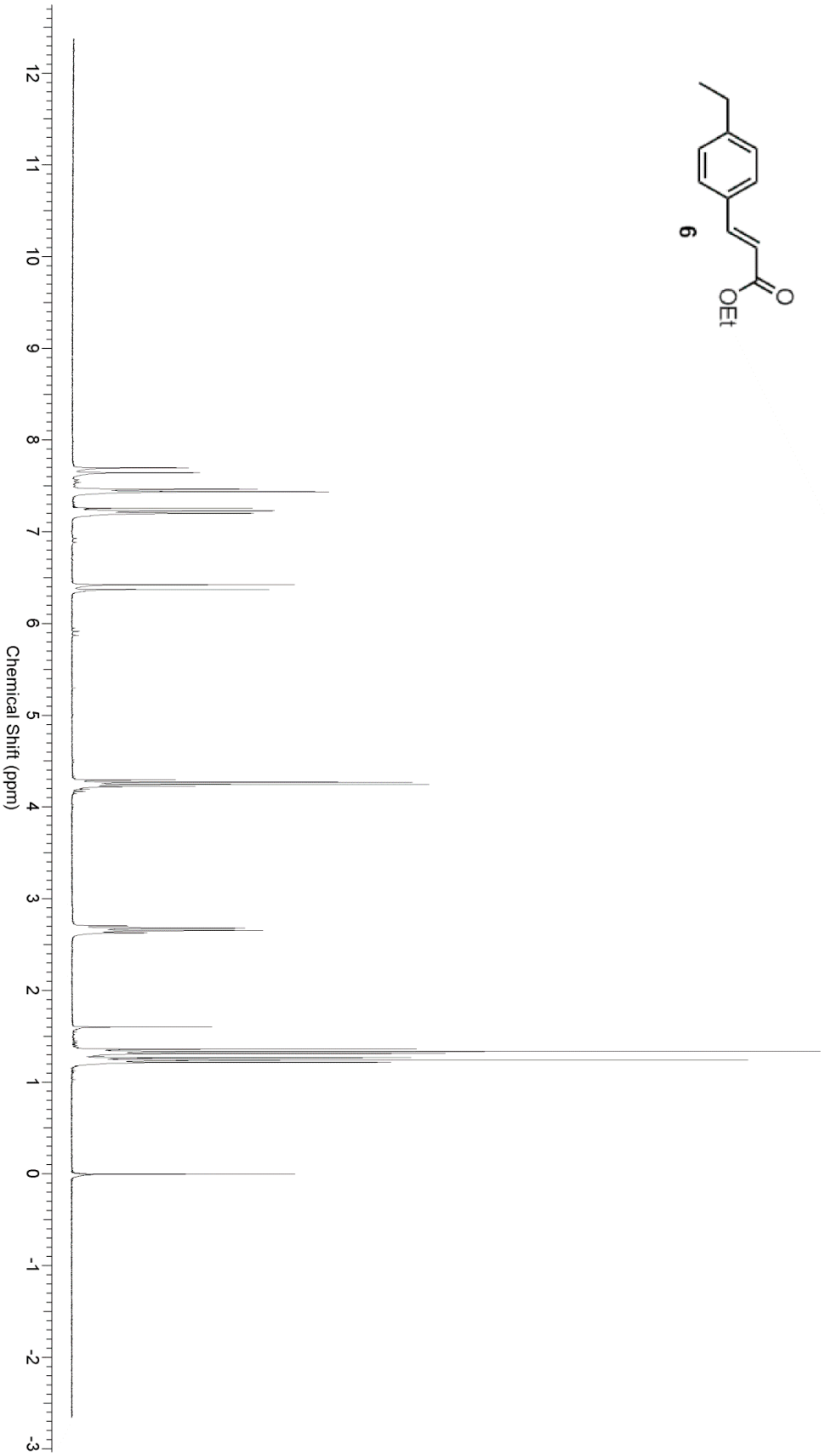

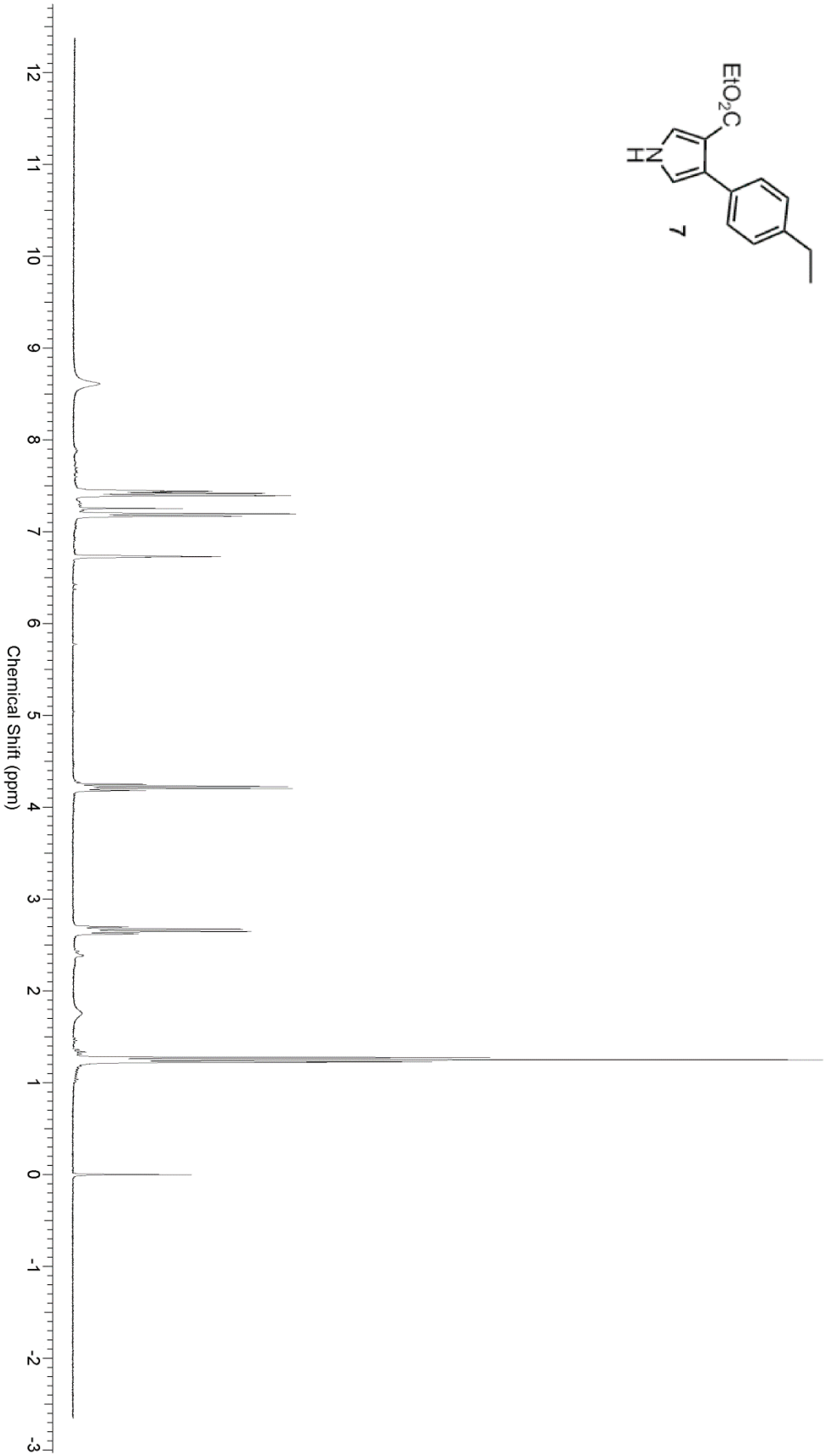

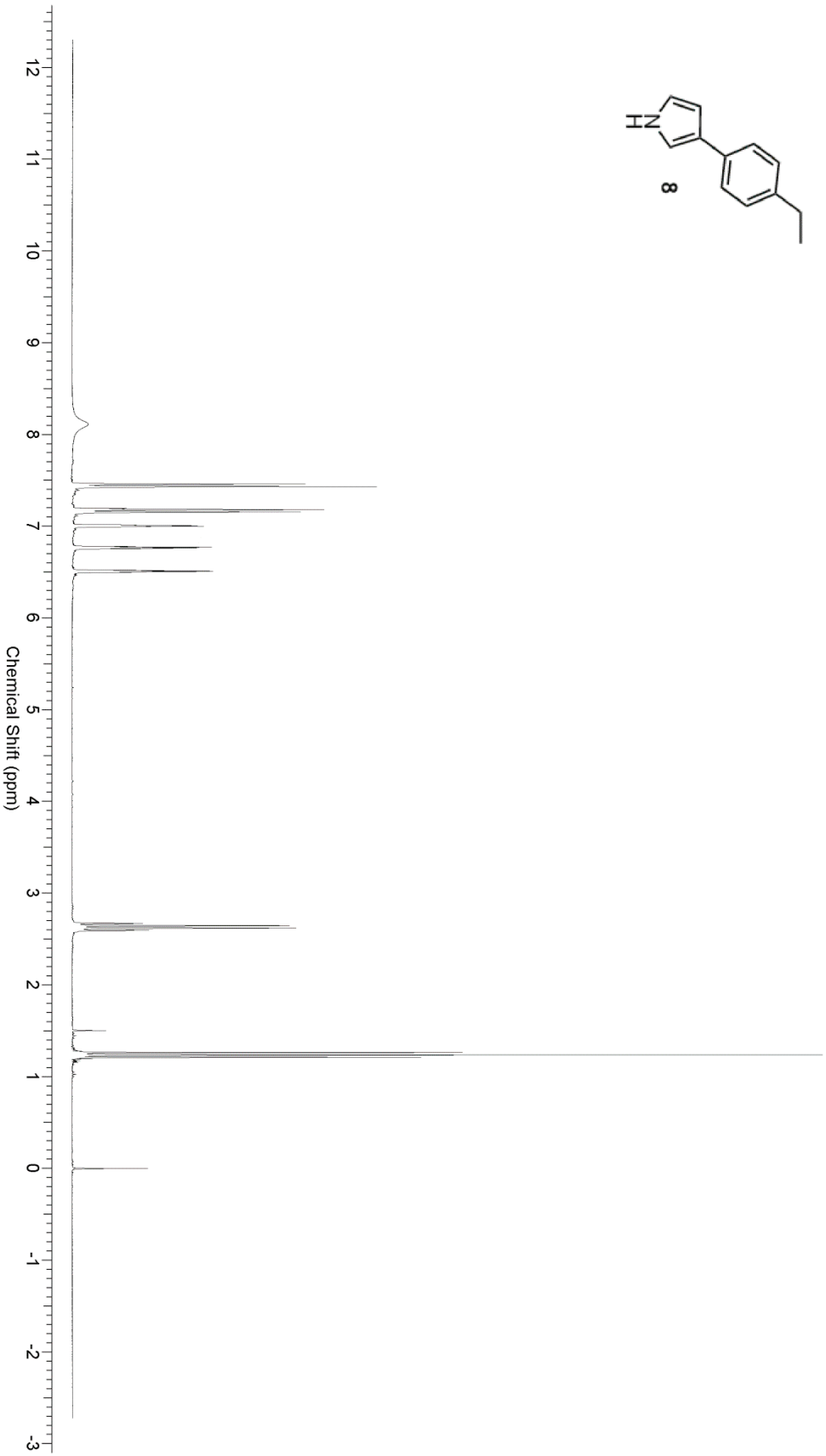

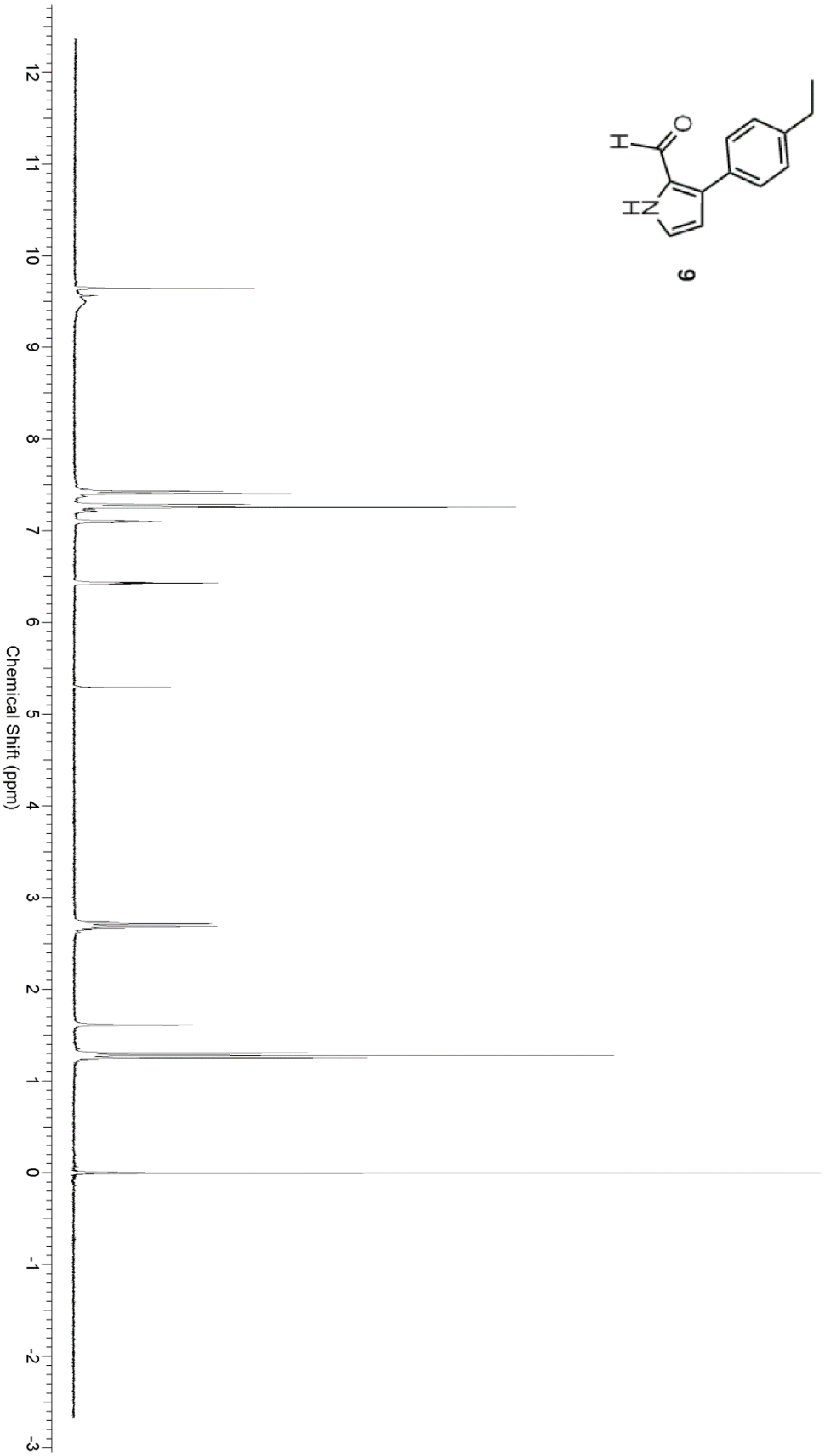

9

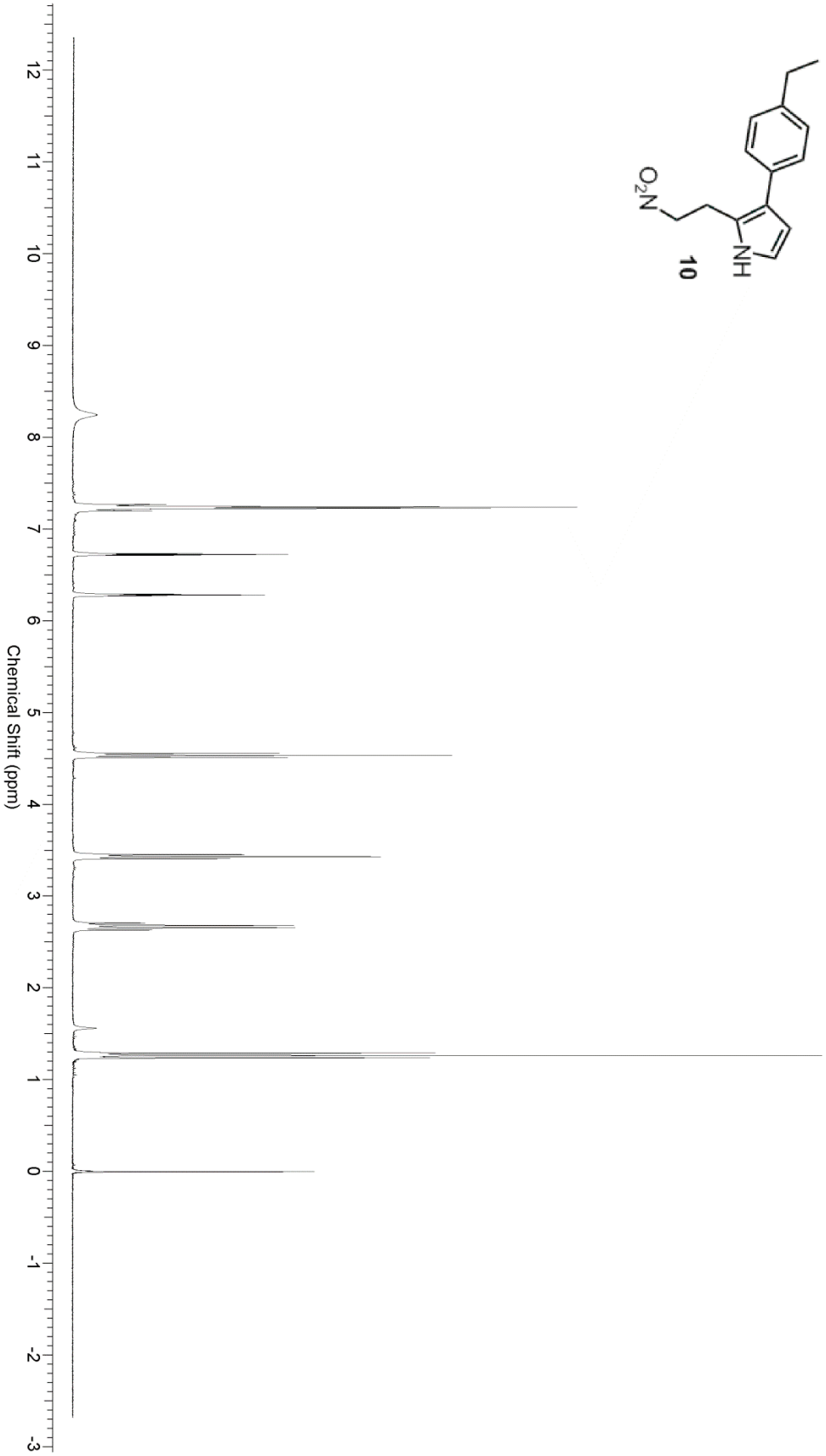

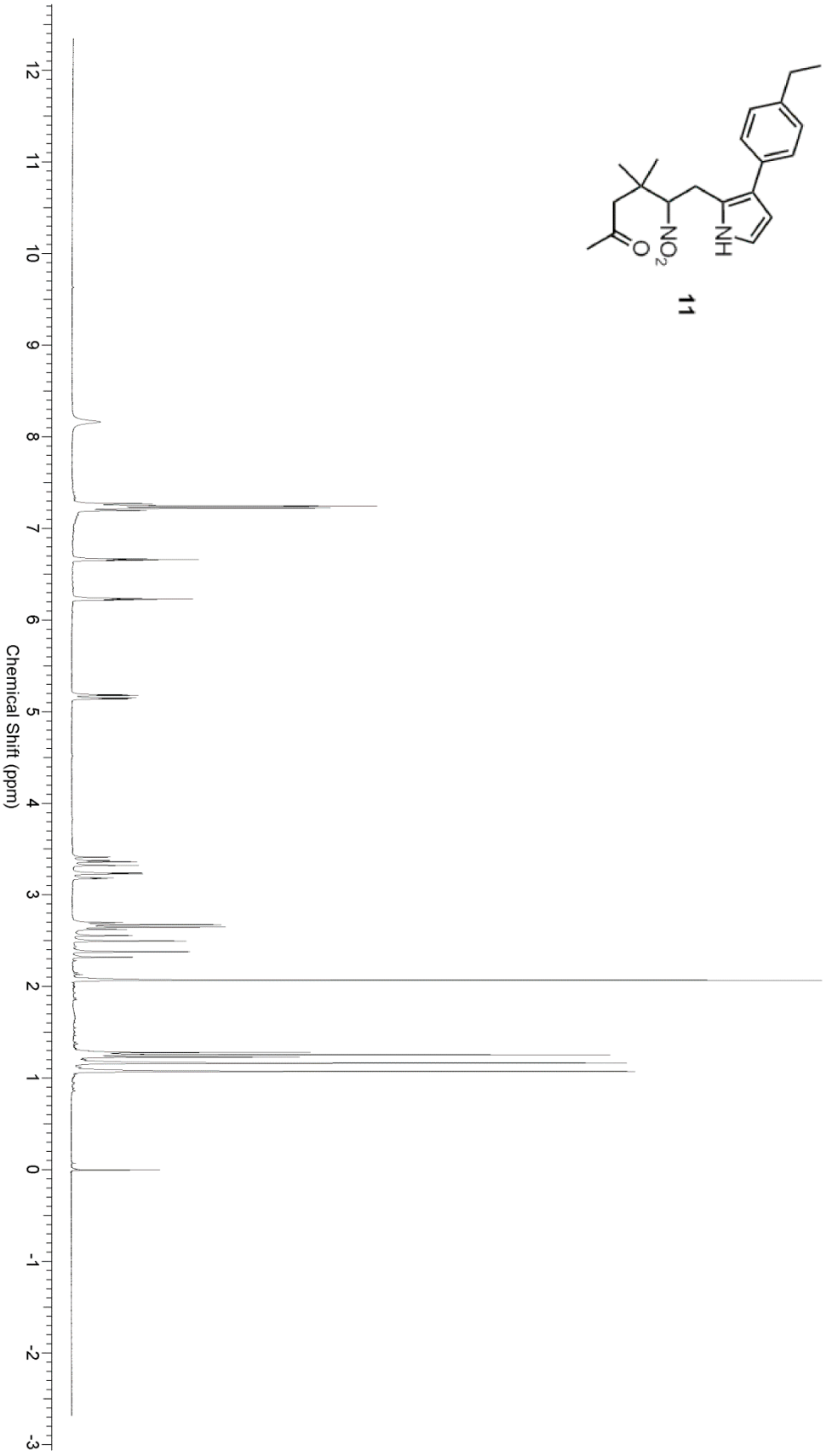

11

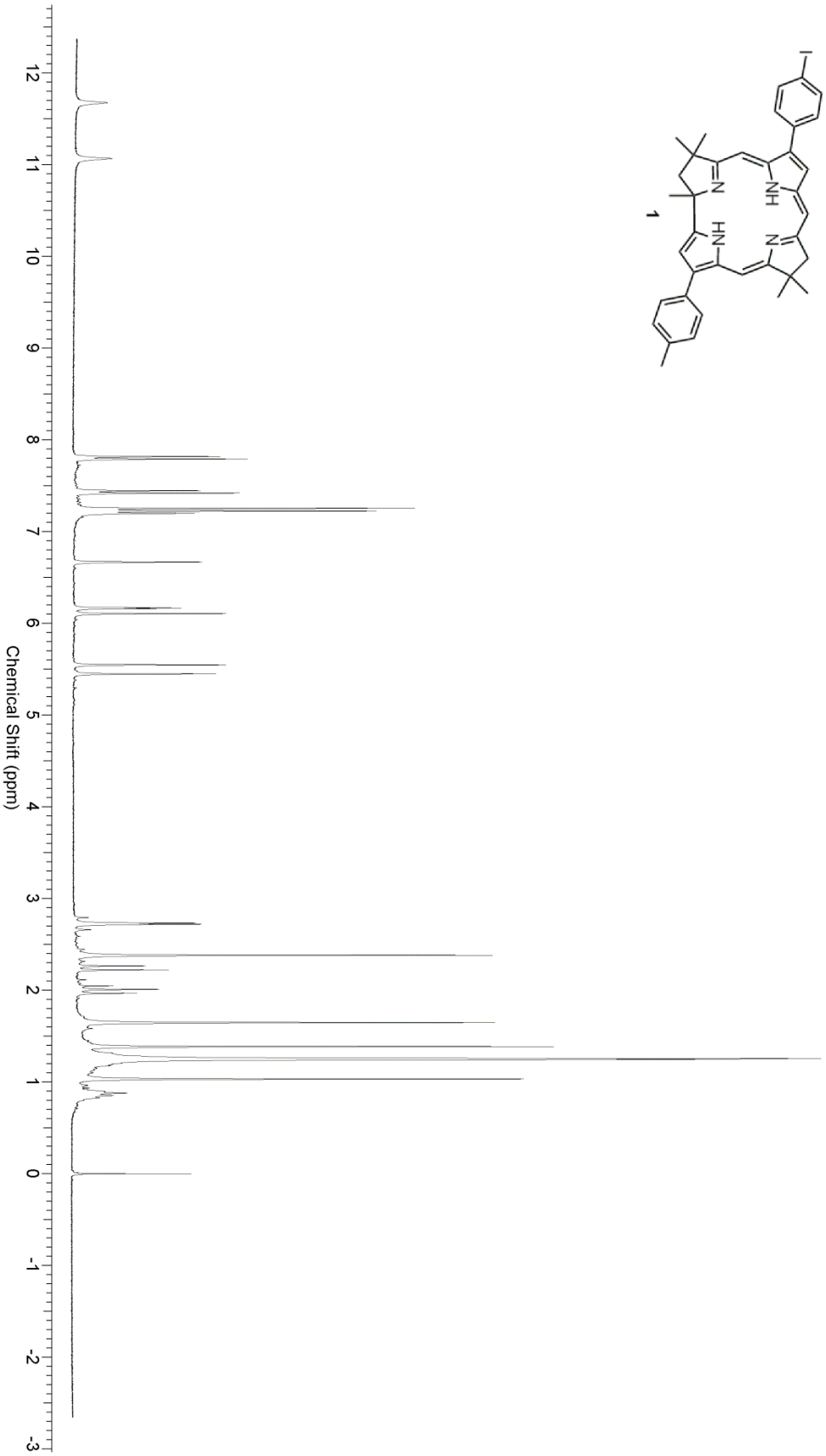

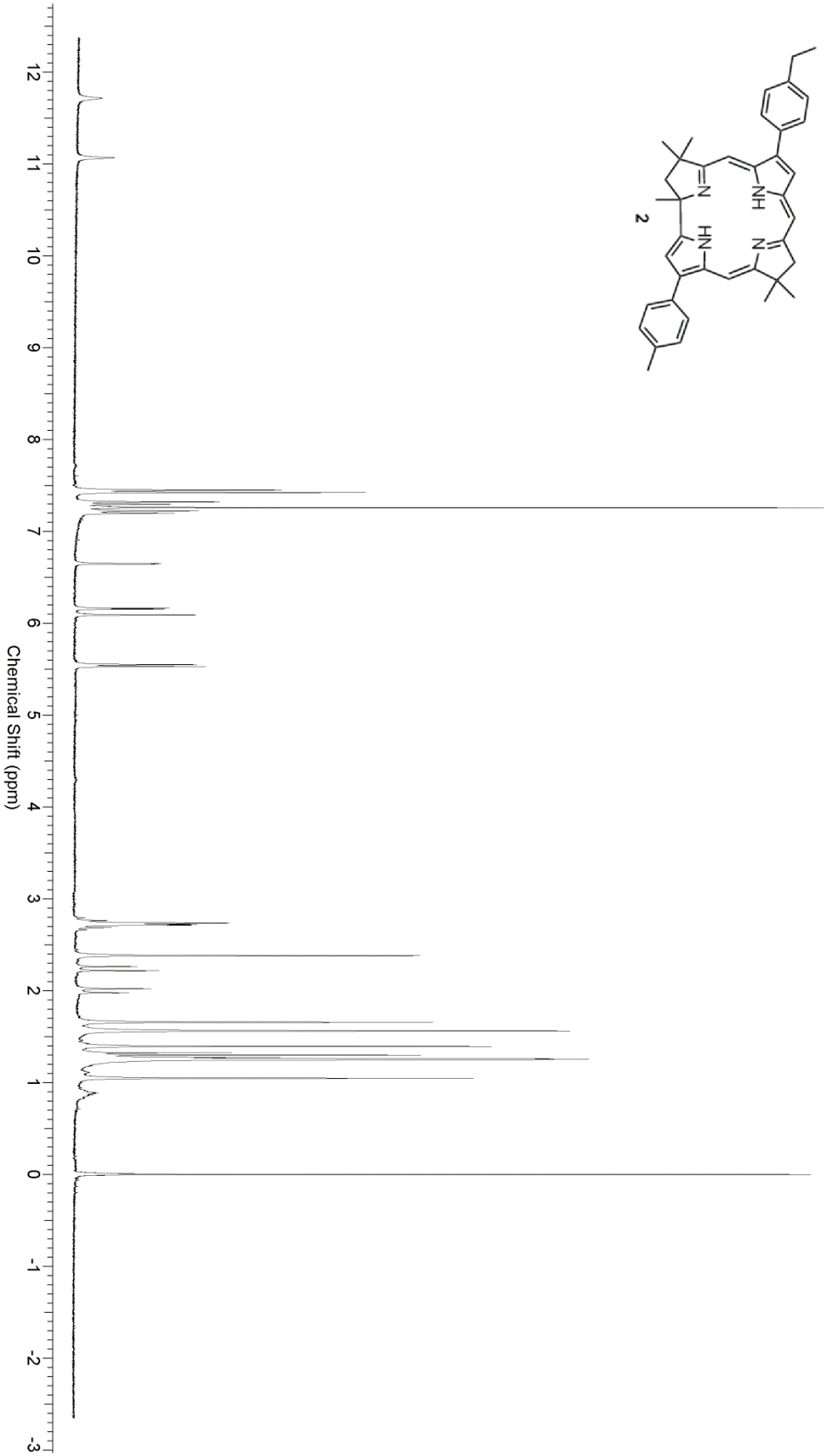

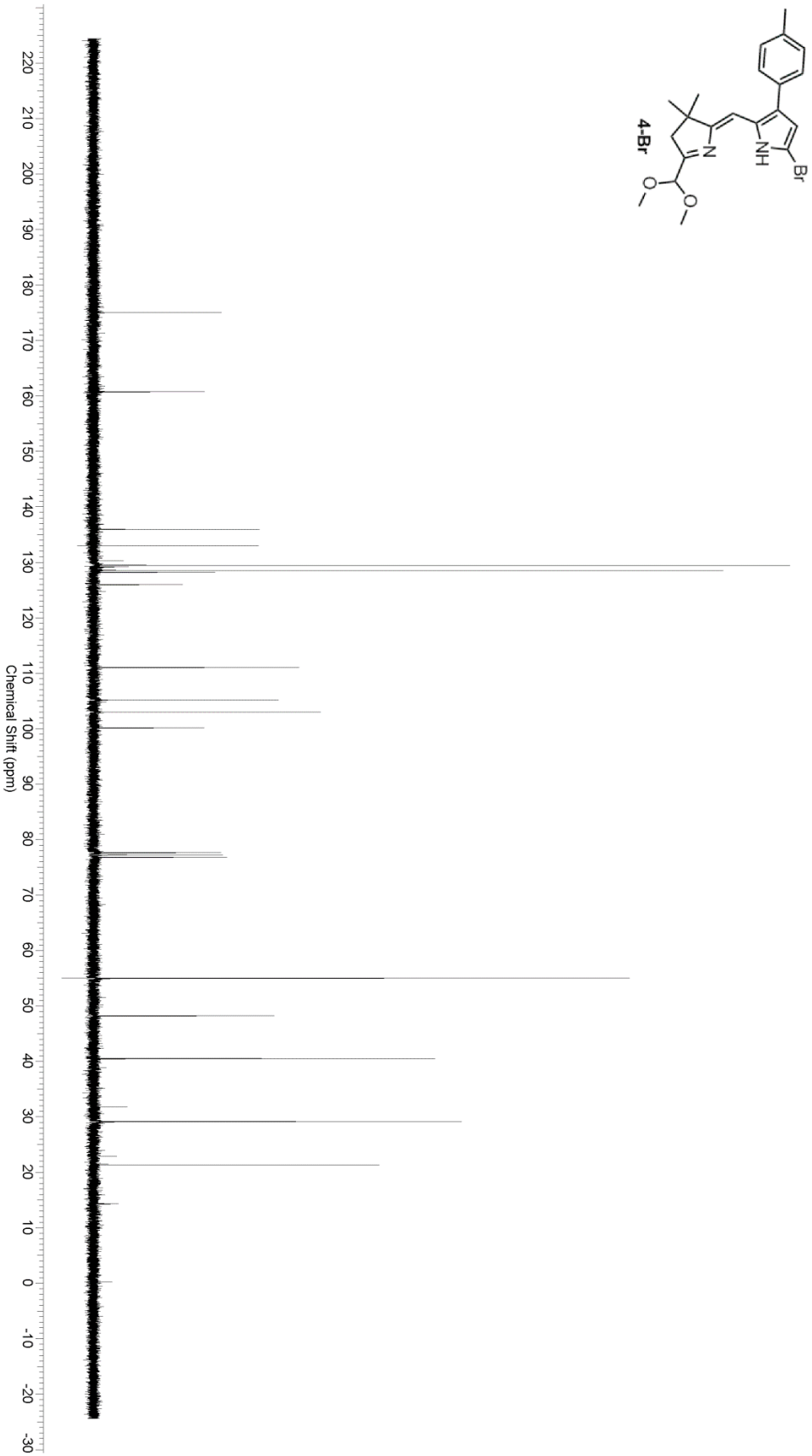

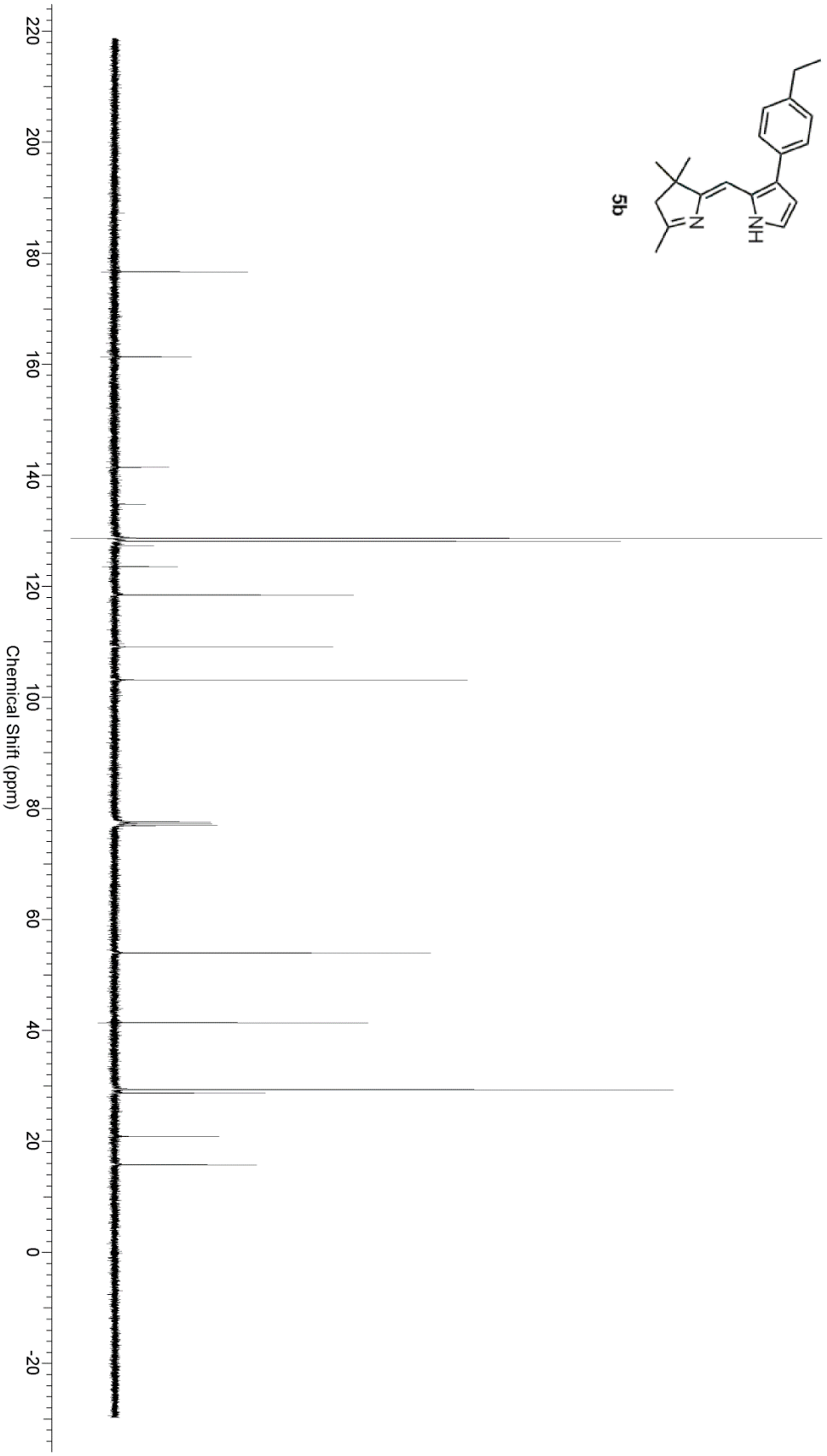

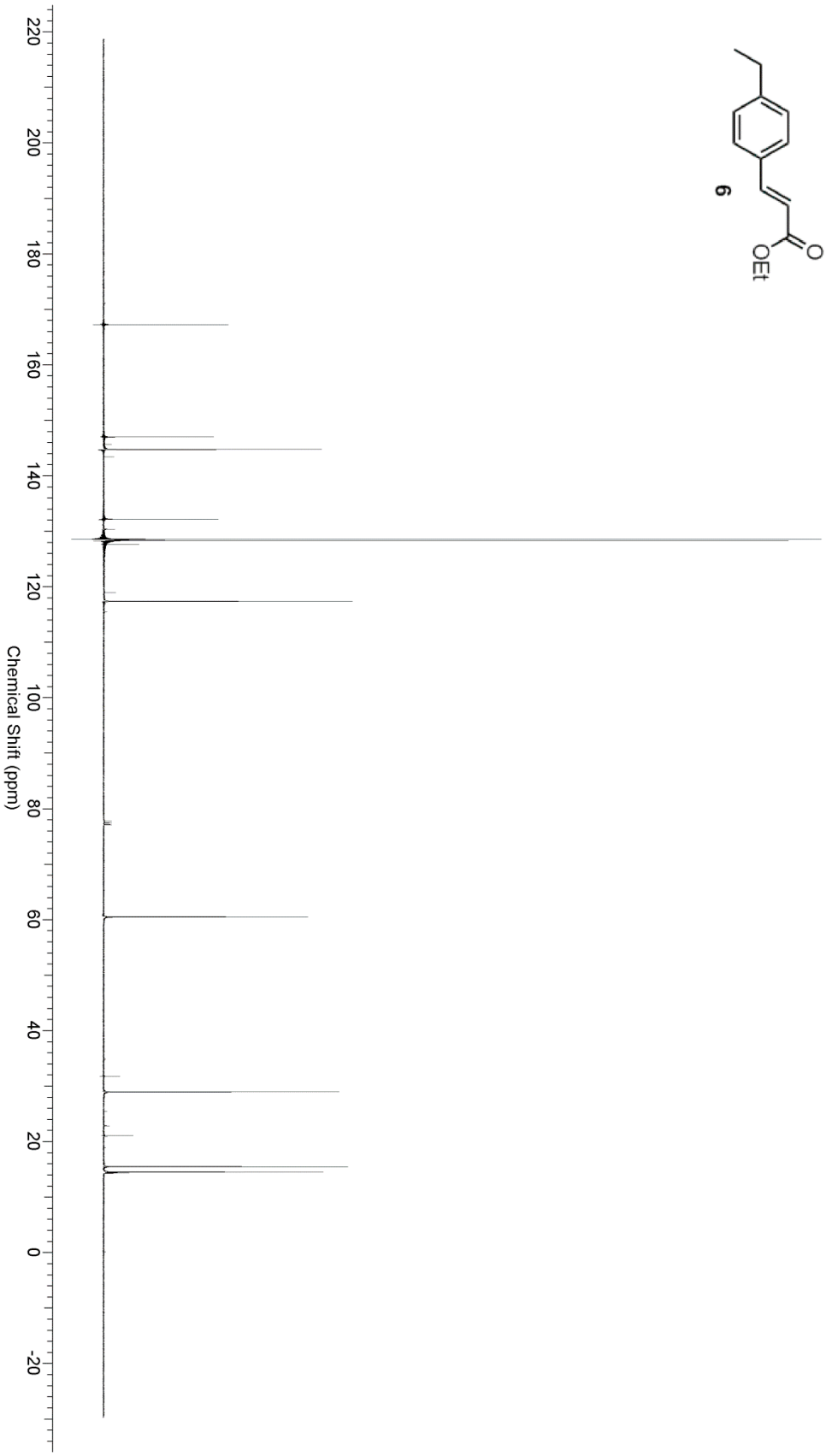

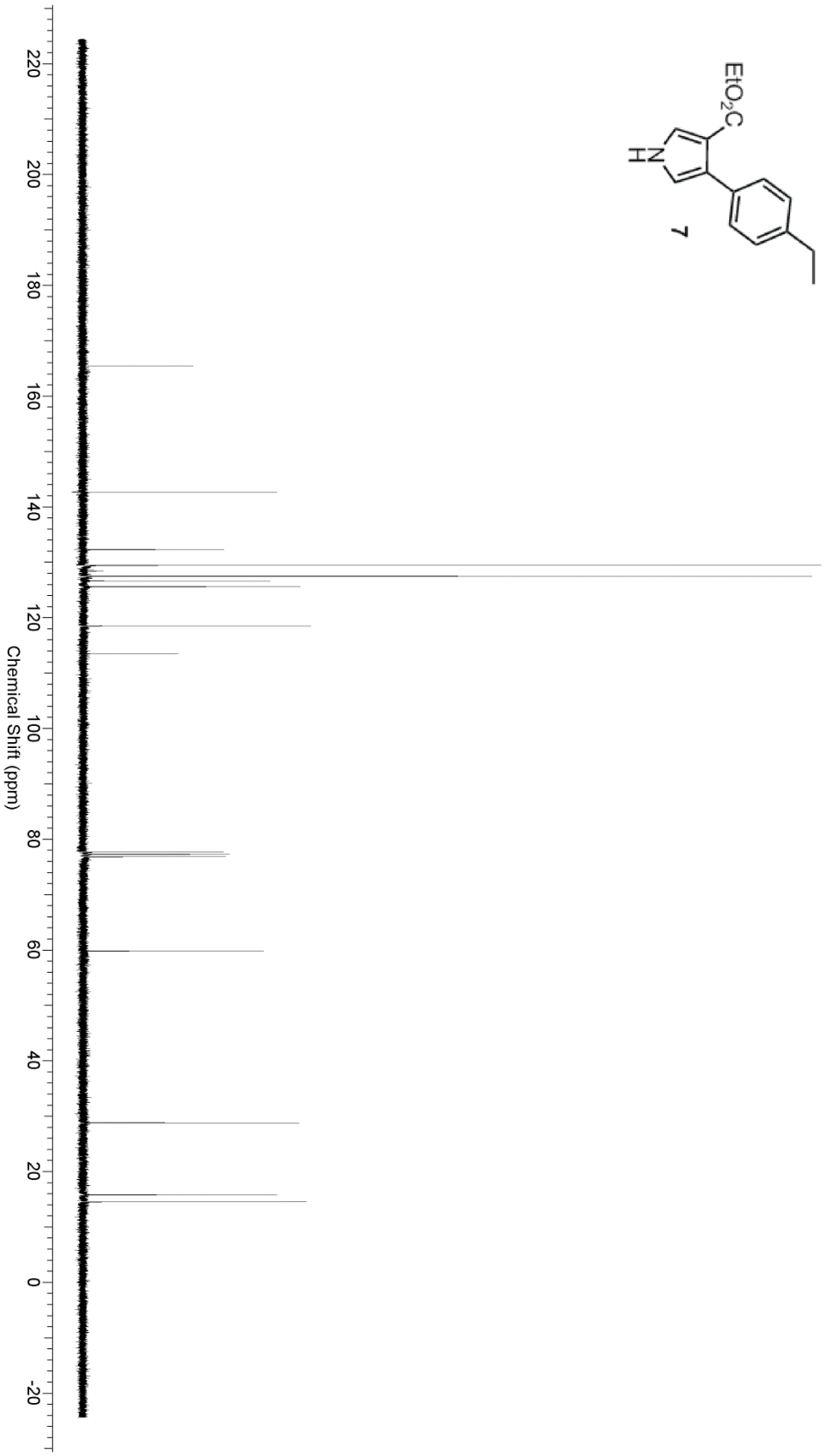

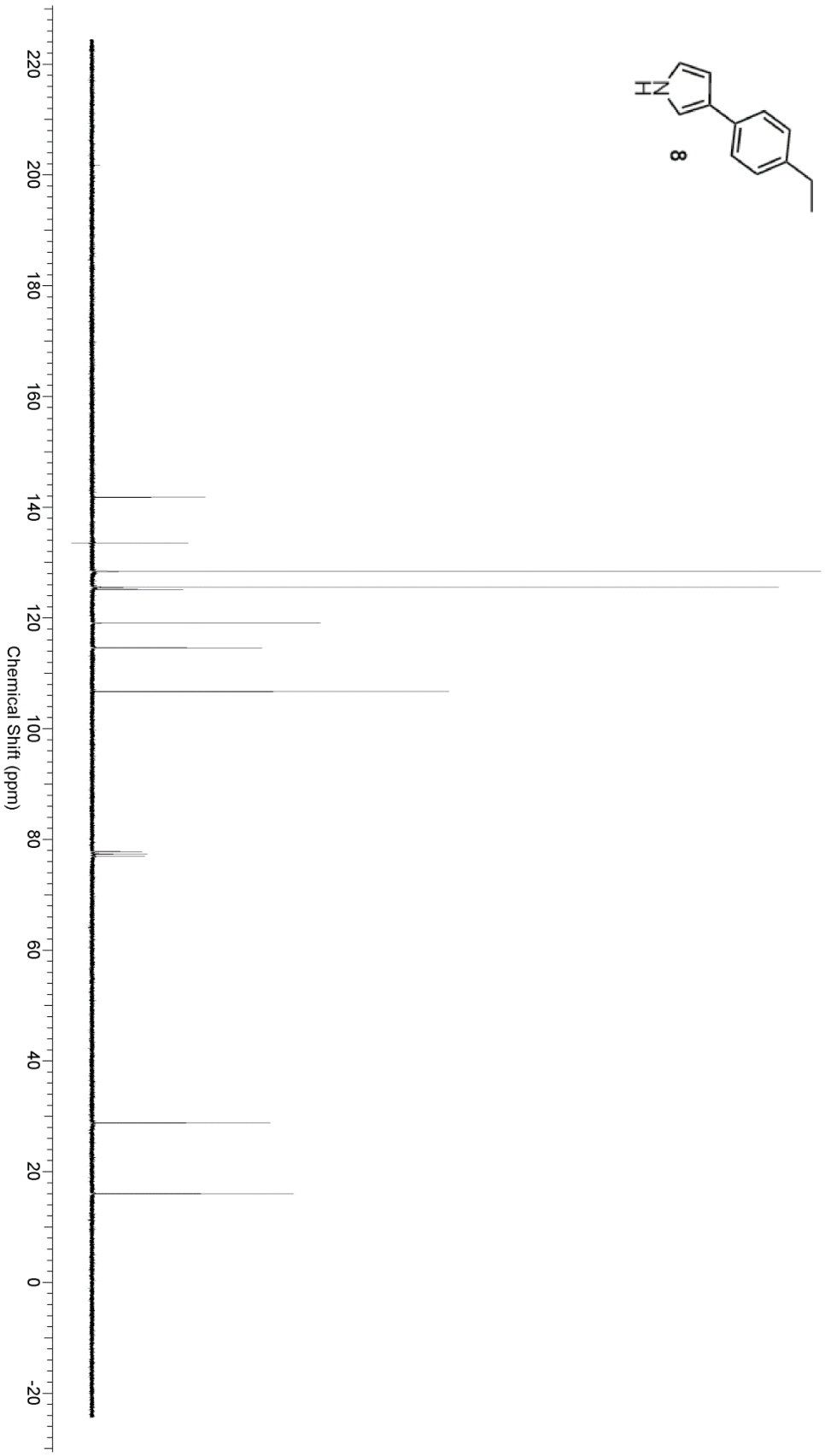

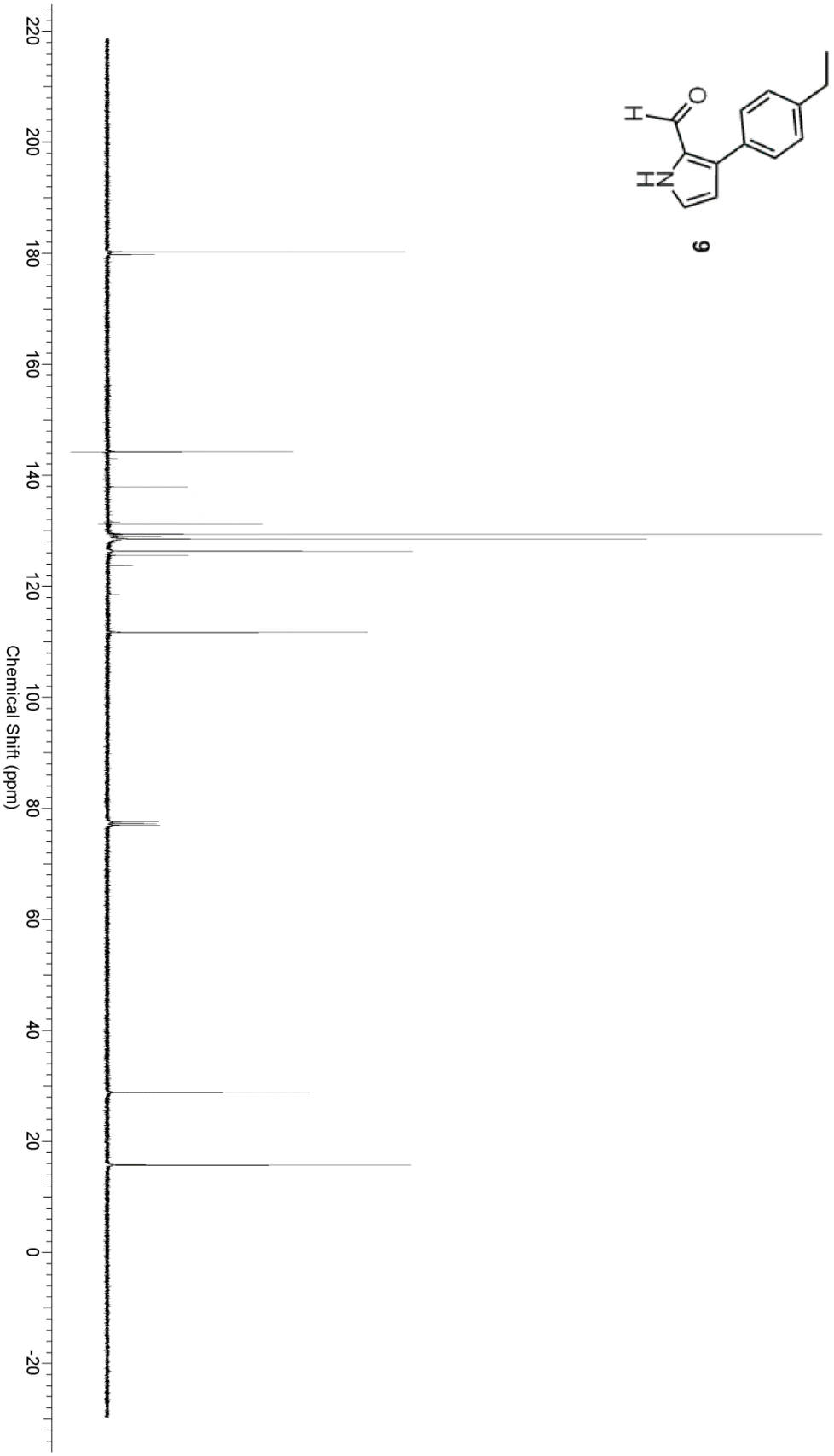

9

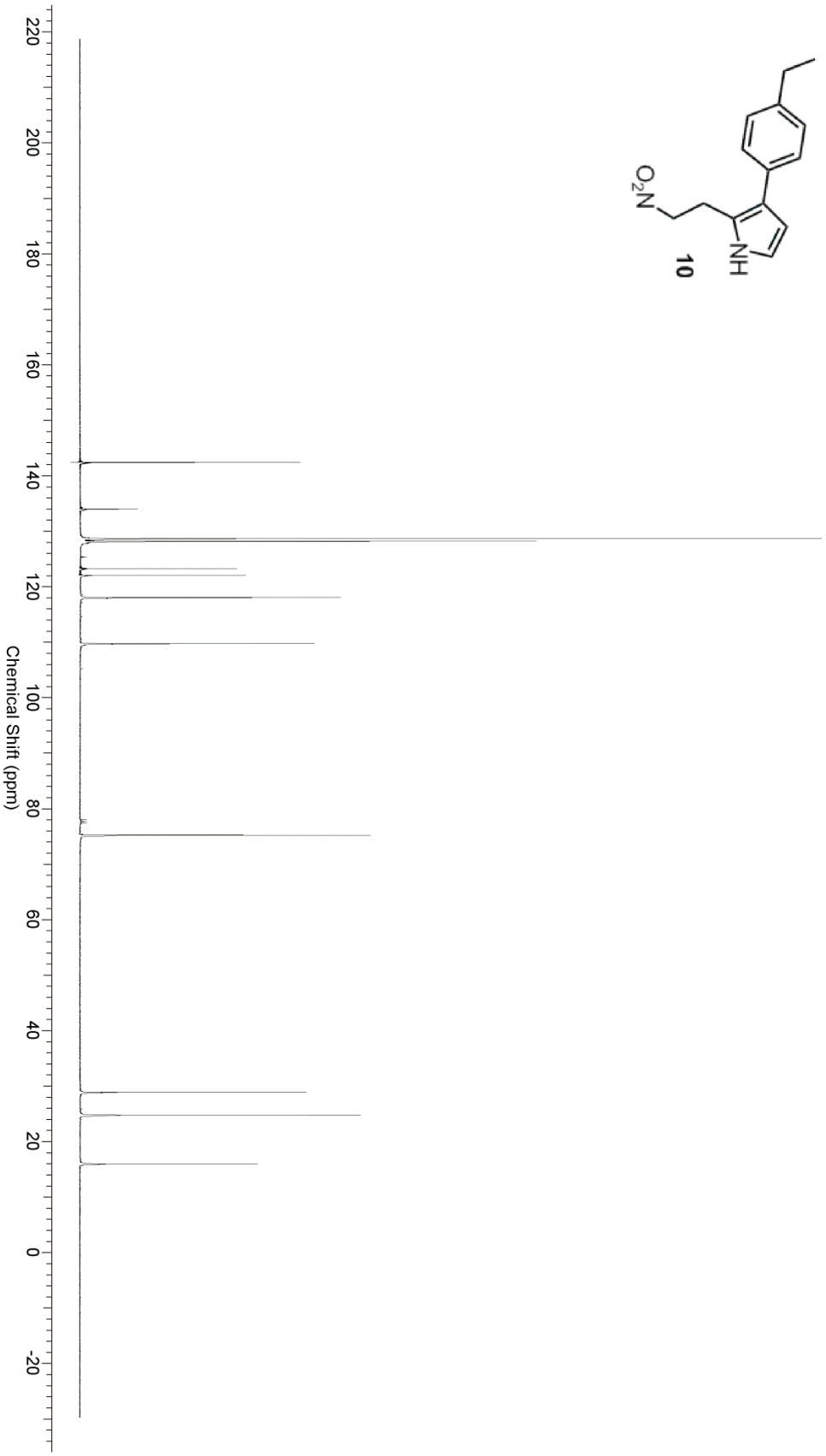

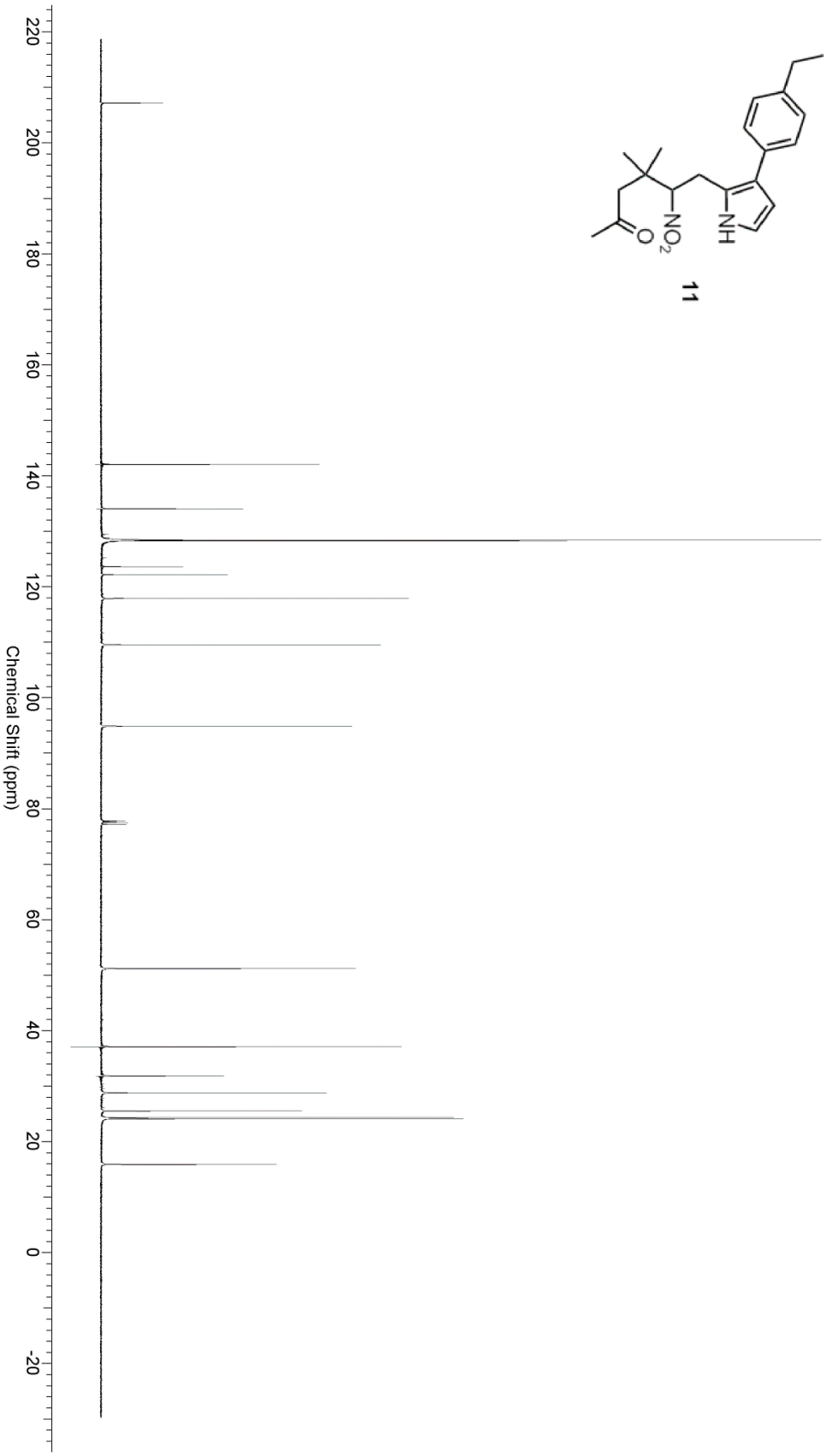

11